

Scaled Down Hydrogen Production in Palladium-Based Membrane Reactors: Process Design and Experimental Investigations

Michael Shoham Patrascu

PhD thesis extended abstract

Technion - Israel Institute of Technology, Haifa, Israel

Abstract

This research is focused on understanding and developing intensified scaled-down H_2 production processes using Pd membrane reactors, via numerical simulations and experimental campaign. We explore the options of using solar energy and biofuels as inputs. This work aims to have an impact on how hydrogen is produced in a decentralized manner, on-site and on-board, enabling its use in fuel cell based cars and other applications. Principles from Process Intensification (PI) are used, namely units integration, to scale down and intensify the traditional process creating an entirely new, low footprint and efficient process.

The computational study, design and operation of two scaled down systems are reported. One system is a heated membrane reformer, intended to be used as on-site production process of pure H_2 . Use of solar power is desired, requiring to lower the operating temperature from ≈ 1000 °C to ≈ 500 °C, which is achieved in the integrated membrane reactor. This work also contributes to elucidate the apparent permeance inhibition effect exhibited in Pd membrane reformers. It is evident that the measured H_2 flux is much lower (up to 80% less) than expected considering the nominal membrane permeance, as measure under pure H_2 conditions. It is demonstrated how model based PI exposes this very important aspect, which could direct future research in the field.

In a second system we investigate on-board production of hydrogen. We propose, design, simulate and demonstrate a highly integrated autothermal reformer. We integrate several unit operations (two reactors, heat exchanger and membrane separation) in one compact system. We investigate the feasibility of exclusively using the the steam reforming effluents as source of heat, and accomplish that by recycling the effluents into a separated packed bed reactor where they are oxidized with air. Hot spots formed in the oxidation chamber (that would significantly lower the overall efficiency), are mitigated by axially distributing the recycled oxidation feed to create an isothermal temperature profile. We demonstrate production of pure atmospheric pressure H_2 , rather than using vacuum or sweeping gas, outperforming most previously published systems. Another important result of this work is the feasibility of operating the same system with various fuels; natural gas or liquid biofuels. Expressing such flexibility is extremely important for the future energy market, and has not been thoroughly reported previously. This design is a proof of concept for on-board pure H_2 generators, with flexible fuel sources, and holds a great promise to eliminate the need for expensive H_2 transport and storage technologies for portable or stationary applications.

1 Introduction

The world is showing an increasing interest in H₂ production as feed to proton exchange membrane (PEM) fuel cells, owing to the breakthroughs in fuel cell technology in the late 1990s. Conventionally H₂ is produced mainly by methane steam reforming (SR), Eq. (1a), conducted in packed bed tubes filled with Ni based catalyst which are placed in a furnace supplying the heat of reaction by burning fuel. Full conversion of methane to syngas (mixture of CO and H₂) is obtained at typical operation conditions of 25 bar and temperatures as high as 1000 °C. This unit is followed by sequential high and then low temperature water-gas-shift (WGS), Eq. (1b), to produce as much H₂ as possible. These steps are followed by pressure swing adsorption for CO₂ removal and methanation (reverse MSR) for clearing any residual CO [11].



Adopting this large-scale production scheme (typically at scales of 10⁵ Nm³/h) to supply H₂ for distributed electrical power production in PEMFC is challenged by significant complications concerning hydrogen compression, transportation, and storage. Special infrastructure would be required to supply pure H₂ to a small-scale end user, either stationary or portable, with major safety and economic concerns. Thus, intensified efficient decentralized processes are sought.

Membrane reactors (MR), comprising Pd or Pd-Ag thin membranes to separate the hydrogen from the reacting mixture, are a promising way to enable Process Intensification (PI) of small scale, local production of H₂ [4]. These membranes are known to hold essentially infinite selectivity for hydrogen (selectivities were reported to be > 10³ [2]). Their use in reactors has been investigated in the last two decades, introducing advantages such as pure H₂ production in one step with equilibrium shift at lowered temperatures; see recent reviews in [13, 5].

Moreover, alternative sources for H₂ production are desired, with lower (or zero) carbon footprint, such as biofuels; methanol, ethanol, or glycerol (which is a biodiesel production by-product). In this work we take such fuels into account.

The Pd membranes' flux follows Sieverts' law, where the driving force for H₂ transport is with respect to the square root of H₂ partial pressure due to H₂ dissociation on the Pd surface:

$$Q_m = A_m \exp\left(\frac{-E_m}{RT}\right), \quad J_m = \Theta Q_m \left(\sqrt{P_{\text{H}_2}^{\text{ret}}} - \sqrt{P_{\text{H}_2}^{\text{perm}}}\right), \quad (2)$$

where Q_m is the membrane's *permeance* (measured under pure H₂ conditions), J_m is the H₂ flux, $P_{\text{H}_2}^{\text{ret}}$ and $P_{\text{H}_2}^{\text{perm}}$ are the H₂ partial pressures on the retentate and permeate sides respectively, the factor Θ expresses the permeance inhibition by coadsorbates [7] and A_m and E_m are empirical membrane constants. This research is focused on model based PI of H₂ production in Pd membrane reactors, and investigates two methods of decentralized production. This is done by numerical simulations and experimental campaign.

The first part of the work is an effort to build a membrane methane reformer that is heated by solar energy through molten salt [6], thus we limit the wall temperatures to 530 °C, showing that operation is possible in the range of 440-525 °C. A special attention in the modeling effort is given to the various aspects that are unique to a membrane reactor, namely membrane inhibition, concentration polarization, thermal effects and kinetic rateat

Evidently, most of the work on membrane reactors for H₂ production has focused on electrically heated, almost isothermal, systems, *e.g.* [1, 3]. This configuration poses meaningful drawbacks: First, the system has to be connected to the electric grid, and thus unable to support portable or isolated remote applications (transportation, offshore drilling rigs, cellular antennas, etc.). Second, a loss of thermal efficiency is inevitable since methane conversion is limited when the permeate side is at atmospheric pressure and the unconverted methane is lost with the effluents. A scaled down autothermal unit for the production of H₂ from hydrocarbons should couple the endothermic SR with a heat source and increase thermal efficiencies which, in turn, implies increased conversion beyond closed-system equilibrium. This can be achieved by process intensification in membrane reactors, as we demonstrate here in a second *autothermal* system.

This part of the research aims to develop a multifuel autothermal system that can be operated with different fuels with no structure or components change. We experimentally validate our theoretical investigation of such systems, and show that the autothermal operation is feasible solely by recycling and oxidizing the reforming effluents (without any additional fuel or power at steady state). The main reaction in the oxidation reactor is methane oxidation, Eq. (3). While some papers have discussed the need for distributed O₂ feed theoretically [15], experimental demonstrations of this configuration are missing. Here we explore this challenging mode of operation, and demonstrate the first proof-of-concept system [14].



2 Methods

2.1 Mathematical model

Material and energy balances are written in a dimensionless form for the reforming zone (retentate), Eqs. (4) and (5) respectively. This is a 1D transient model which takes dispersion (of heat and chemical species), convection and reaction terms into account.

$$\frac{\partial y_i}{\partial \tau} = \frac{1}{Pe_c} \frac{\partial^2 y_i}{\partial \zeta^2} - \left(\frac{\partial \mathcal{F}}{\partial \zeta} y_i + \frac{\partial y_i}{\partial \zeta} \mathcal{F} \right) + \frac{1}{M_f} \sum_{j=1}^3 \alpha_{i,j} r_j - \frac{\kappa_i y_{\text{CH}_4,0}}{Pe_m} \left(\sqrt{y_i} - \sqrt{Pr y_i^{perm}} \right), \quad (4)$$

$$\frac{t_T}{t_R} \frac{\partial \theta}{\partial \tau} = \frac{1}{Pe} \frac{\partial^2 \theta}{\partial \zeta^2} - \frac{\partial \theta}{\partial \zeta} + \frac{1}{E_f} \sum_{j=1}^3 (-\Delta H_j) r_j - \mathcal{U}(\theta - \theta_w), \quad (5)$$

where y_i are the components' mole fractions, θ is the normalized temperature, τ and ζ are the normalized time and space respectively, $\kappa_i = 1$ for H₂ and 0 for the other components (assuming infinite membrane selectivity), r_j are the reactions rates and Pr is the ratio of the pressures in the retentate and permeate. More details on the model are given in [9, 10]. The important dimensionless parameter is Pe_m , which is defined as the ratio of methane feed flow rate to a maximum flow of H₂ through the membrane, accounting for the total membrane area and zero inhibition ($\Theta = 1$):

$$Pe_m = \frac{F_{\text{CH}_4,0}}{\pi d_m L Q_m \sqrt{P}}. \quad (6)$$

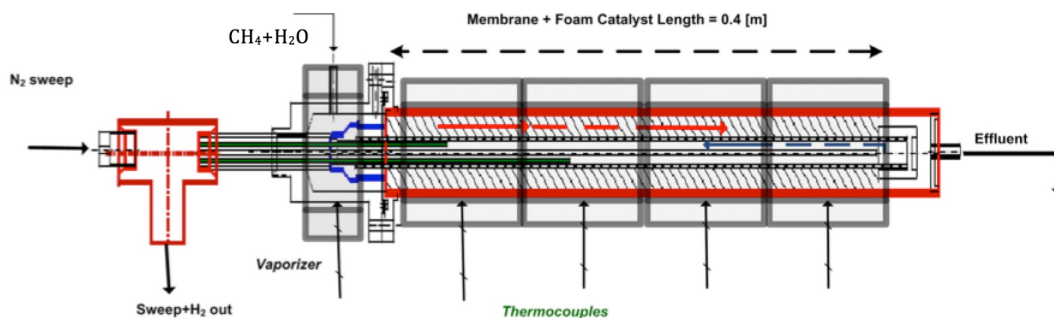


Figure 1: Detailed drawing of the heated membrane reformer. The 4 electric heaters are shown as transparent bodies around the reactor tube (red). Five outer thermocouples are shown (as electronic signal arrows) as well as 2 (of total 4) inner thermocouples (green).

For a specific reactor configuration, this number is reversely proportional to the total membrane area used, thus it has the same significance as GHSV in traditional catalytic reactors.

The dynamics in the above equations is less important for the heated reformer, but is very important to simulate the autothermal configuration, discussed in the sequel, which may exhibit moving thermal fronts and extinction.

2.2 Heated membrane reformer

The heated membrane reactor is built as a tube and shell like structure, Figure 1. In the shell side 8 half annular cylinders of Ni-Pt/CeO₂ foam catalyst are placed, with a total length of 0.4 m. The membrane tube provided by ECN (Hysep-technology) is made of a 4-5 μm palladium layer, 175 cm² in surface area. Inside the membrane an 1/8" stainless steel tube supplies the sweep flow, in counter current to the reactive flow. Four concentric electric heaters are placed around the reactor, each is controlled independently to maintain a set temperature measured on the outer wall of the reactor.

2.3 Autothermal membrane reformer

The autothermal system suggested here, couples a membrane reformer for atmospheric pressure H₂ production by SR with an oxidation (Ox) reactor supplying the heat of reforming, constructed as a shell and tube architecture as depicted in Figure 2. The design incorporates full recycle of the SR effluents and their mixing with air before entering the Ox compartment, to achieve autothermal operation with highest thermal efficiency. The two streams are arranged in a counter-current mode to improve heat recuperation (see Figure 2).

In its cross section the SR and Ox compartments are concentric and four Pd-Ag membranes are placed within the SR reactor. Its axial design includes two sections: (I) Reaction section with heat transfer and hydrogen separation. (II) Heat recuperation section, with no membranes, where the two streams exchange heat and the exit stream leaves at higher temperature than the feed. The permeate side is exposed to atmospheric pressure in all cases, and its flow is measured directly by a mass flow meter.

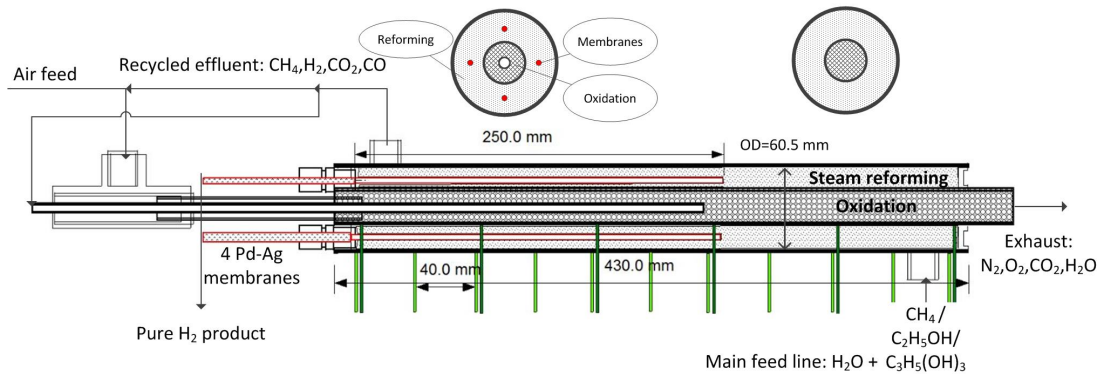


Figure 2: A detailed drawing of the reactor. The cross sections of the two reactor zones are depicted above. The 11 outer and 6 inner thermocouples (green) and two of the four membranes (red in the colored version) are depicted in the axial view. The recycled SR effluents are fed to the internal oxidation reactor in two axial locations using the branch tee (left) and an inner Hasteloy tube. Surrounding electrical heaters for start-up, and the insulation layer are not shown for clarity.

3 Results

3.1 Heated membrane reformer

We first address the results of the heated membrane reformer [10]. The performance of the system is evaluated with respect to the main operating conditions, namely feed flow rate, temperature, pressure, S/C ratio and sweep flow rate. The most important performance parameters to evaluate are CH_4 conversion, $f = \frac{F_{\text{CH}_4,0} - F_{\text{CH}_4}}{F_{\text{CH}_4,0}}$, the permeate flow rate and the H_2 recovery (permeate flow rate vs. the H_2 production rate).

The flow rate is the most important parameter that affects performance. While performance of regular packed bed reactors is presented against the ratio of reaction rate to flow rate (Damköhler number, or simply residence time), performance of membrane reactors are better presented in terms of the Pe_m number, Eq. (6). Unfortunately, this is still not well recognized in the engineering community, and most publications still use GHSV to represent membrane reactors performance. In the limit of very fast reactions the conversion depends on the Pe_m number only [12].

Figure 3 compares simulation results with experimental measurements conducted at methane flow rates of 0.25, 0.5, 0.75 and 1.5 NL/min (GHSV of 136, 272, 408, 816 h^{-1} respectively). High conversion and high H_2 recovery are achieved at low flow rates, then they monotonically decrease. In membrane reactors the conversion is controlled by the membrane transport, especially at low temperatures, which explains the relation between the two. Hydrogen purity of $>99\%$ was measured by GC for all runs reported. The permeate flow rate is $F_{\text{H}_2}^{\text{perm}} \approx 4F_{\text{CH}_0}fX$ (neglecting CO formation), thus as the feed flow rate increases (so does Pe_m for a specific reactor configuration) the permeate flow rate passes through a maximum at relatively low feed flow rates. The (first) asymptotic conversion is the closed system (no membranes) equilibrium conversion which is 22.3% at these conditions. This trend is well predicted by the model (at much higher flow rates the reaction rate will limit the conversion, and it will decline).

Main results obtained are over 90% conversion and 80% hydrogen recovery, for feed flow of

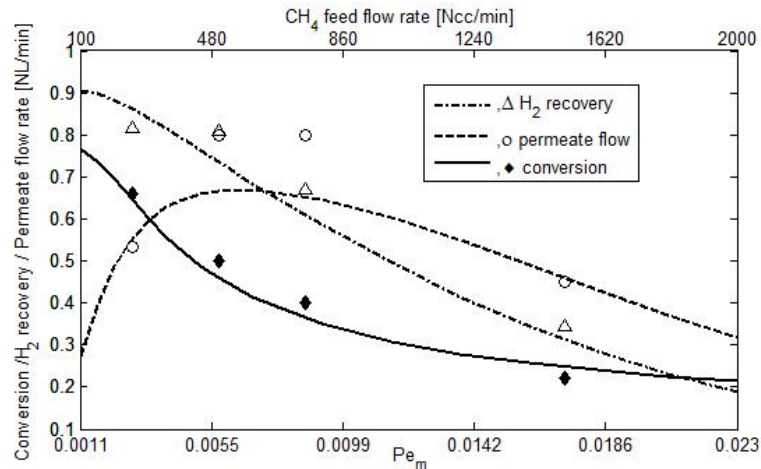


Figure 3: Conversion, permeate flow rate, and H₂ recovery vs feed flow rate ($T_w = 525$ °C, $P=10$ bars, $S/C=3$, no sweep). Lower abscissa indicates Pe_m number and the upper one indicates the corresponding methane feed flow rate. Markers are measurements and lines are simulation results.

0.25 NL/min methane at wall temperature of 525 °C, pressure of 10 bar, $S/C = 3$ and sweep flow of 0.7 NL/min. Exit compositions were mostly very close to equilibrium with respect to measured exit H₂ concentration, which supports our assertion that the kinetic rates are not the controlling step. Hydrogen flux intensification was obtained by increasing retentate (reaction) pressure and by introducing sweep flow of N₂ in the permeate side. Sweep flow is a means of increasing the driving force for H₂ transport across the membrane. The obvious disadvantage is the need for further separation of the H₂ from the sweep. Here we use nitrogen as sweep, while in practice steam will be likely used, making subsequent H₂ separation easier, yet with significant energetic cost. In a solar reformer plant that uses molten salt at ≈ 530 °C the molten salt effluent from the reactor-heat exchanger may be used to generate steam to be used as sweep to increase the driving force for H₂ transport.

An asymptotic permeate flow was observed with increasing pressure (not shown) which was much lower than the expected value, if permeance inhibition is not considered, $\Theta = 1$ (0.85 vs 2 NL/min respectively). Concentration polarization effects are ruled out as a source of this inhibition, by running 2D simulations that are not detailed here. Using the expression derived by Israni et al. [7] and calibrated for Pd-Ag membrane to account for inhibition of H₂O, CO₂ and CO cannot account for the observed permeance inhibition here. We conclude that the inhibition of CH₄ on H₂ transport through Pd membranes must be investigated in mixtures of all relevant species, especially in the presence of H₂O. Our results suggest that in spite of a negligible inhibition attributed to CH₄ by most publications, a significant effect might be present under real steam reforming conditions (presence of H₂O), even when CO concentrations are close to zero.

Further study was conducted on *ethanol* SR in this system [8]. The results of this work show that the combination of the Ni/Pt catalyst and the Pd membrane for hydrogen removal produce very high values of hydrogen yield, despite the low steam to ethanol ratio and the moderate pressure levels.

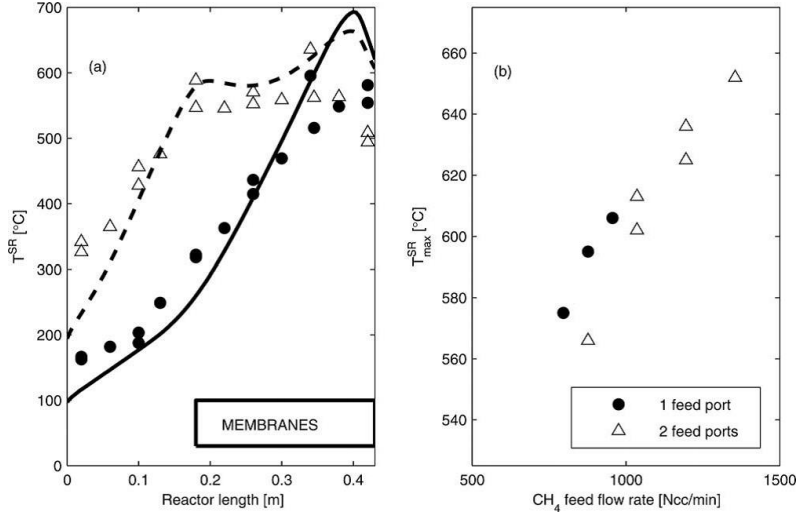


Figure 4: The effect of distributed oxidation feed on temperature profile: (a) Axial temperature profile on the inner tube and outer shell of the MSR reactor for 1 and 2 oxidation feed ports. Simulations (lines), with no adjustable parameters, and measurements (dots) for CH_4 feed flow rates of 880 and 1200 Ncc/min, respectively. The axial position of the membranes is also shown. (b) Maximal measured temperature in the MSR reactor vs. the feed flow rate of methane.

3.2 Autothermal membrane reformer

Membrane reactors' performance is often characterized by the obtained conversion, H_2 recovery and the permeate flow rate. In this integrated system, however, these are not as important individually, thus we choose to focus on the temperature profile, the overall thermal efficiency, Eq. (7), and the equivalent power output of the product, which equals to the numerator in (7). These attributes are equivalent to yield and productivity in traditional reactors. The thermal efficiency is defined as the ratio of the lower heating values (LHV) of the product H_2 supplied by the membrane, to that of the total hydrocarbon fed to the system plus any auxiliary power. The latter includes the duty required to externally evaporate water before feeding and to operate a vacuum pump, however these are not used in our suggested system, thus W_{aux} is zero.

$$\eta = \frac{F_{H_2}^{perm} LHV_{H_2}}{F_{HC}^{in} LHV_{HC} + W_{aux}}. \quad (7)$$

Feed distribution to the oxidation reactor leads to a more uniform temperature profile, almost isothermal along the membranes, and thus higher flow rates can be applied vs the undistributed feed. Figure 4a compares the temperature profiles measured (represented by dots) using one or two feed locations, which were obtained for CH_4 feed flow rates of 880 and 1200 Ncc/min, respectively. The single feed case, where there is only one hotspot near the inlet, is more sensitive in this respect (Ox feed is to the right in Figure 4a). Because the temperature is not an independent variable in this mode of operation (of using only the recycled SR effluent as heat source), and cannot be controlled independently, the maximal temperature (T^{max}) is monotonically increasing with feed flow rate, Figure 4b, as more fuel is combusted.

Obviously, operating conditions should be such that maintain the autothermal system in the ignited state. Since the main component that is recycled to the combustion reactor is methane

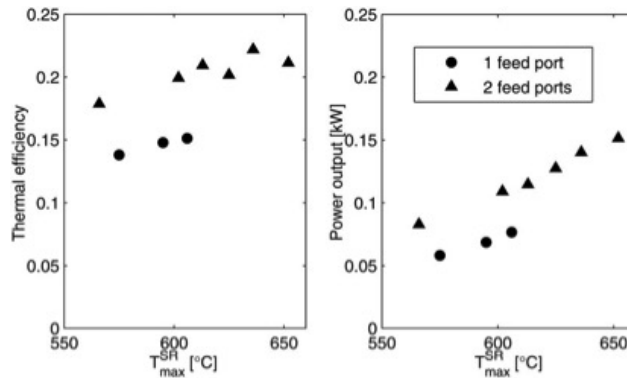


Figure 5: The effect of distributed oxidation feed on the reactor’s performance; thermal efficiency (left) and equivalent power of H_2 product (right) vs. the maximal measured MSR reactor temperature. Methane as fuel, $S/C = 2$, $P = 11$ bar.

(true even when biofuels are used as inputs), which is the most difficult hydrocarbon to oxidize, we expect that the system will undergo extinction when the (maximal) reaction temperature falls below ≈ 500 °C, the temperature required for methane combustion.

Normally the membranes’ tolerable operating temperature limits these systems, and thus it is a good practice to compare their performance with respect to the maximal temperatures measured. Figure 5 shows that the efficiency in the two-port feed case is 30-40% better than that in the single-port feed when compared at the same maximal temperature (*e.g.* at 600 °C). Furthermore, splitting the feed improves the pure H_2 flow rate by 40-50%.

The measurements are adequately predicted by the simulation results without adjustable parameters but while accounting for permeance inhibition both by competitive adsorption and concentration polarization, Figure 6. The membranes’ permeance inhibition plays a significant role here as well, as evident by comparing the methane feed case to the predicted theoretical performance assuming no inhibition, $\Theta = 1$.

We have demonstrated in Figure 6 that the performance improves monotonically as feed flow rate increases. This is an opposite trend to the one demonstrated for the heated membrane reformer. The reason is that the temperature increases with increasing feed rate, because it is an auto thermal system with full recycle, and temperature is not controlled independently. For very high feed flow rates the SR conversion and the H_2 recovery should decrease (in this system the increase in temperature is compensating over this effect). In the asymptotic case the permeate flow rate will be negligible, and the system will reduce to a simple combustion reactor, producing only heat. Thus, we expect an optimal temperature to exist, however, much higher than the feasible operating temperature of the membranes.

4 Conclusions

The performance of a methane and ethanol membrane steam reformer, packed with a 175 cm^2 high-flux Pd membrane and a foam catalyst, was investigated in the low temperature range of 440-525 °C. An appropriate mathematical model, with two adjustable parameters (permeance and heat transfer) predicts the results well. The experimental results, which reflect reduction in permeance of 80% when compared with that in pure H_2 , were best predicted when adsorption of

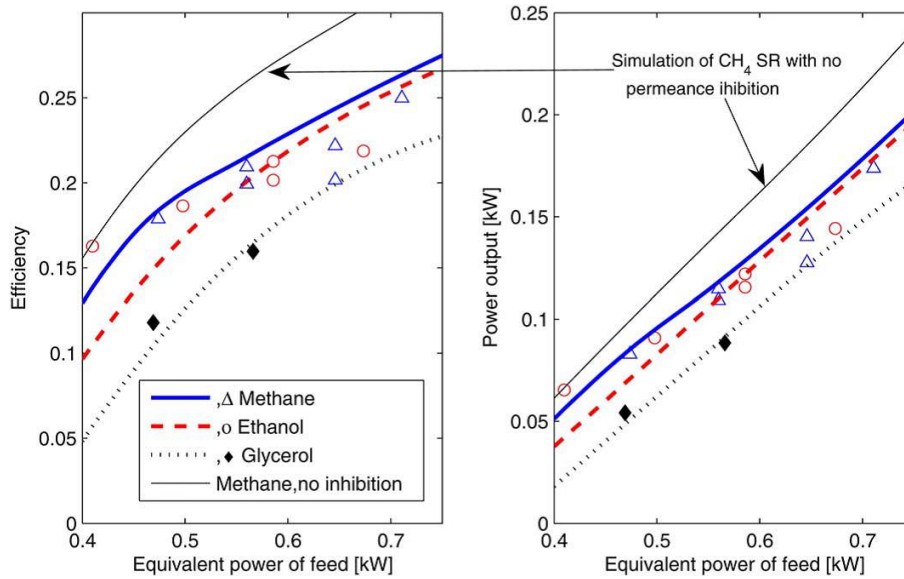


Figure 6: The autothermal system’s performance for different fuels fed vs. the inlet fuel’s equivalent power. Thermal efficiency (left) and equivalent power of H₂ product (right). Markers are experimental measurements and lines are model predictions. The case of methane as feed assuming no inhibition of the membranes permeance is plotted for reference and shows a significant effect.

CH₄ was considered as strong as that of CO. This apparent permeance inhibition is attributed to coadsorbates, although the only strong inhibitor in these conditions is thought to be CO and its concentrations (< 1%) cannot justify this strong inhibition.

We have successfully demonstrated, for the first time to our best knowledge, the intensified production of pure atmospheric pressure H₂ in a compact integrated autothermal membrane reactor fed by a variety of fuels or biofuels. Feeds of methane, ethanol, or glycerol and stoichiometric steam were considered with heat supplied solely by recycling the SR effluents to an internal combustion reactor after mixing with air.

Still the efficiencies of the lab scale system are about 25% at best. Noting that around 50% of the energy is lost to the surroundings, we expect that increasing membrane area and applying better insulation will push the efficiencies to 60% as was simulated in [10]. Achieving efficiencies better than 60% will open the door, we believe, to consider this process as superior energetically, when coupled with FC (with efficiencies that are claimed to be 60%), over the simple direct combustion of these fuels (with ICE efficiencies that are expected to be 30%).

References

- [1] A. Basile, S. Campanari, G. Manzolini, A. Iulianelli, T. Longo, S. Liguori, M. De Falco, and V. Piemonte. Methane steam reforming in a Pd-Ag membrane reformer: An experimental study on reaction pressure influence at middle temperature. *Int. J. Hydrogen Energy*, 36(2):1531–1539, 2011.
- [2] Y. Chen, Y. Wang, H. Xu, and G. Xiong. Hydrogen production capacity of membrane

- reformer for methane steam reforming near practical working conditions. *J. Memb. Sci.*, 322(2):453–459, 2008.
- [3] B. Dittmar, a. Behrens, N. Schödel, M. Rüttinger, T. Franco, G. Straczewski, and R. Dittmeyer. Methane steam reforming operation and thermal stability of new porous metal supported tubular palladium composite membranes. *Int. J. Hydrogen Energy*, 38(21):8759–8771, 2013.
- [4] E. Drioli, A. I. Stankiewicz, and F. Macedonio. Membrane engineering in process intensification An overview. *J. Memb. Sci.*, 380(1-2):1–8, sep 2011.
- [5] F. Gallucci, E. Fernandez, P. Corengia, and M. van Sint Annaland. Recent advances on membranes and membrane reactors for hydrogen production. *Chem. Eng. Sci.*, 92:40–66, 2013.
- [6] A. Giaconia, L. Turchetti, G. Monteleone, B. Morico, G. Iaquaniello, K. Shabtai, M. Sheintuch, D. Boettge, J. Adler, V. Palma, S. Voutetakis, A. Lemonidou, M. C. Annesini, M. Den Exter, and H. Balzer. Development of a solar-powered, fuel-flexible compact steam reformer: The CoMETHy project. *Chem. Eng. Trans.*, 35(1):433–438, 2013.
- [7] S. H. Israni and M. P. Harold. Methanol Steam Reforming in PdAg Membrane Reactors: Effects of Reaction System Species on Transmembrane Hydrogen Flux. *Ind. Eng. Chem. Res.*, 49(21):10242–10250, 2010.
- [8] M. A. Murmura, M. Patrascu, M. C. Annesini, V. Palma, C. Ruocco, and M. Sheintuch. Directing selectivity of ethanol steam reforming in membrane reactors. *Int. J. Hydrogen Energy*, 40(17):5837–5848, 2015.
- [9] M. Patrascu and M. Sheintuch. Design concepts of a scaled-down autothermal membrane reformer for on board hydrogen production. *Chem. Eng. J.*, 282:123–136, dec 2015.
- [10] M. Patrascu and M. Sheintuch. On-site pure hydrogen production by methane steam reforming in high flux membrane reactor: Experimental validation, model predictions and membrane inhibition. *Chem. Eng. J.*, 262:862–874, 2015.
- [11] J. Rostrup-Nielsen. *Concepts in syngas manufacture*. Imperial College Press, 2011.
- [12] M. Sheintuch. Design of Membranal Dehydrogenation Reactors: The Fast Reaction Asymptote. *Ind. Eng. Chem. Res.*, 37(3):807–814, 1998.
- [13] Shigarov, Meshcheryakov, and Kirillov. Use of Pd membranes in catalytic reactors for steam methane reforming for pure hydrogen production. *Theor. Found. Chem. Eng.*, 45(5):595–609, 2011.
- [14] M. Shoham Patrascu and M. Sheintuch. Multi-fuel scaled-down autothermal pure H₂ generator: Design and proof of concept. *AIChE J.*, 62(6):2112–2125, jun 2016.
- [15] T. P. Tiemersma, C. S. Patil, M. van Sint Annaland, and J. A. M. Kuipers. Modelling of packed bed membrane reactors for autothermal production of ultrapure hydrogen. *Chem. Eng. Sci.*, 61(5):1602–1616, 2006.